VOL. 9, NO. 9, SEPTEMBER 2014 ISSN 1819-6608
ARPN Journal of Engineering and Applied Sciences


www.arpnjournals.com

NEW MODEL FOR ELLIPTICAL FLOW REGIME IN HYDRAULICALLY-FRACTURED VERTICAL WELLS IN HOMOGENEOUS AND NATURALLY-FRACTURED SYSTEMS

Freddy Humberto Escobar[1], Alfredo Ghisays-Ruiz[2] and Luis Fernando Bonilla[1]
[1]Universidad Surcolombiana/CENIGAA, Avenida Pastrana - Cra 1, Neiva, Huila, Colombia
[2]Universidad del Atlantico, Fac. de Ciencias Básicas. antigua vía Puerto Colombia, Barranquilla, Atlantico, Colombia
E-Mail: fescobar@usco.edu.co

ABSTRACT

Pressure tests in infinite-conductivity hydraulically-fractured vertical wells allow for the estimation of the actual half-fracture length. If only elliptical flow is observed then the knowledge of the drainage area is required for the analysis which could lead to have a longer test for observing late psudosteady-state regime. Sometimes, it is unpractical to do so, then a new elliptical model excluding the reservoir area for the half-fracture length estimation is presented in this work for both homogeneous and naturally-fractured occurding hydrocarbon formations. *TDS* technique and conventional analysis were implemented for characterizing this flow regime. The resulting equations were successfully tested with synthetic pressure tests.

Keywords: pressure transient analysis, fracture conductivity, fracture half-length, *TDS* technique, homogeneous systems, naturally fractured reservoirs.

1. INTRODUCTION

The pressure behavior of horizontal and hydraulically-fractured vertical wells is very similar. The difference is that the later has two wings and covers the complete formation thickness. Then, elliptical flow regime is expected to be observed during early time of transient pressure tests in both cases.

The elliptical flow regime was originally neglected in horizontal wells and it was treated as a transition period. The first research found on this issue was provided by Isaaka *et al*. (2000) who characterized such flow regime and identified it on the pressure derivative curve by a slope of 0.35. Chacon, Djebrouni and Tiab (2004) presented a new pressure derivative equation for this flow regime which depends upon the reservoir length along the *x*-direction, reservoir thickness, horizontal wellbore length, well radius and horizontal reservoir permeability.

Later Escobar, Muñoz and Sepulveda (2004) obtained the governing pressure equation by integrating the model presented by Chacon *et al*. (2004). They developed analytical equations to obtain horizontal permeability anisotropy. The intersection points of the elliptical-flow regime with early-linear, early-radial, late-linear and/or late-linear flow regimes have also been used to find new analytical expressions to verify the horizontal permeability or to find the permeability in the *y*-direction. They applied the *TDS*, Tiab (1993), methodology for characterizing the elliptical flow regime so new equations using characteristic lines and points found on the pressure and pressure derivative plot were developed to obtain areal permeability, $(k_x k_y)^{0.5}$, the reservoir length along the *x*-direction, h_x, permeability in the *y*-direction, k_y, and the geometrical skin factor, $s_{Ell,}$ caused by the convergence from early-linear flow to elliptical flow regime. Escobar and Montealegre (2008) using also the model developed by Chacon *et al*. (2008), implemented the conventional-straight line method for characterizing the elliptical flow regime, so the reservoir areal permeability and elliptical skin factor can be estimated.

However, Chacon *et al*. (2004)'s model fail sometimes to provide accurate values of horizontal permeability, then, Martinez, Escobar and Bonilla (2012) reformulated the model and provided both conventional straight-line and *TDS* methods as interpretation techniques for crude and gas flow. For the latter case, they used both real time and pseudotime functions.

Tiab (1994) was the first who found this flow regime in pressure test data of infinite-conductivity hydraulically fractured vertical wells. He called it as "birradial flow", provided the governing pressure and pressure derivative equations and implemented the *TDS* technique for its characterization.

Although Tiab's model, Tiab (1994), works perfectly, it requires the knowledge of well-drainage area for estimating the half-fracture length. However, sometimes this condition cannot be met because the pressure test needs to be run long enough for the development of the late time pseudosteady state for the determination of the drainage area. Then, a new model excluding the reservoir drainage area is presented here and successfully tested with synthetic examples. Also, Tiab's model, Tiab (1994), is slightly modified here to account for naturally-fractured double-porosity systems.

2. MATHEMATICAL FORMULATION

2.1. Basic equations

The dimensionless time quantities based upon half-fracture length, drainage area and reservoir width, respectively, are given below:

$$t_{Dxf} = \frac{0.000263kt}{\phi\mu c_t x_f^2} \quad (1)$$

$$t_{DA} = \frac{0.000263kt}{\phi\mu c_t A} \quad (2)$$

$$t_{DL} = \frac{0.000263kt}{\phi\mu c_t Y_E^2} \quad (3)$$

The dimensionless pressure and pressure derivative parameters for oil reservoirs are given by:

$$P_D = \frac{kh\Delta P}{141.2q\mu B} \quad (4)$$

$$t_D * P_D' = \frac{kh(t*\Delta P')}{141.2q\mu B} \quad (5)$$

Finally, the dimensionless fracture conductivity introduced by Cinco-Ley, Samaniego and Dominguez (1976) is defined as:

$$C_{fD} = \frac{k_f w_f}{k\, x_f} \quad (6)$$

2.2. Governing equations

Gringarten, Ramey, and Raghavan (1974) presented the solutions of the difussivity equation for a vertical well drainage by infinite-conductivity or uniform-flux vertical fracture. Later, Tiab (1994) introduced the governing equation of the birradial flow regime dominating the early time behavior during the acting of an infinite-conductivity fracture.

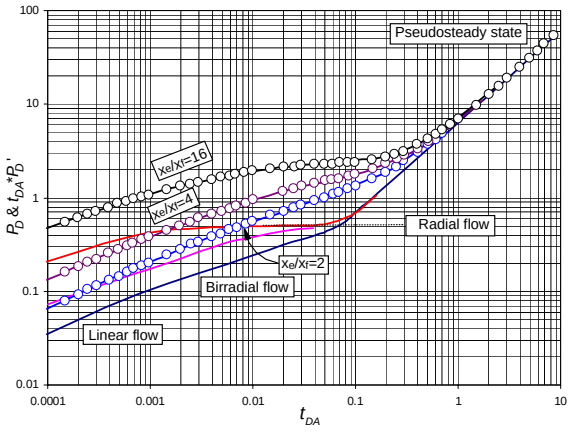

Figure-1. Dimensionless pressure and pressure derivative vs. dimensionless time based on area for a vertical well with an infinite-conductivity fracture well, after Tiab (1994).

As presented by Tiab (1994) for the case of an infinite-conductivity fractured well, the linear flow regime becomes shorter as the x_e/x_f ratio increases. When this ratio is higher than 16, linear flow regime is no longer observed and birradial flow regime dominates the early time data. Based on these criteria, Tiab (1994) presented the governing equation for birradial flow regime,

$$P_D = 2.14\left(\frac{x_e}{x_f}\right)^{0.72}\left(\frac{t_{DA}}{\xi}\right)t_{DA}^{0.36} \quad (7)$$

Notice that ξ was original excluded in Tiab's model since it was only presented for homogeneous formations. When ξ = 1, Equation (7) accounts for homogeneous reservoirs. For the case of naturally-fractured formations, $\xi = \omega$ which is the dimensionless storativity coefficient. The above expression, although it is correct, presents a major drawback in cases where the pressure test is not long enough to reach the reservoir boundaries. In such cases, the drainage area is unknown and Equation (7) has no applicability.

Figure-2 shows the dimensionless pressure and pressure derivative versus dimensionless time based on fracture length. Linear flow regime is observed at early time in the test. After a short transition, the birradial flow regime is observed. A new expression excluding reservoir drainage area is presented here,

$$P_D = \frac{25}{9}\left(\frac{\pi t_{Dxf}}{26\xi}\right)^{0.36} \quad (8)$$

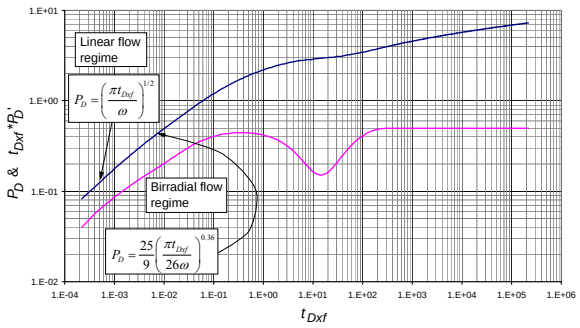

Figure-2. Dimensionless pressure and pressure derivative behavior for an infinite-conductivity fractured vertical well in a heterogeneous reservoir, $\lambda = 1x10^{-8}$ and $\omega = 0.1$.

As for the case of Equation (12), Equation (13) applies to either homogeneous or heterogeneous (double porosity) systems. Again, for homogeneous systems the ξ value is either dropped or set equal to the unity. The pressure derivative of Equation (8) is given as,

$$t_D * P_D' = \left(\frac{\pi t_{Dxf}}{26\xi}\right)^{0.36} \quad (9)$$

After plugging the dimensionless parameters given by Equations (1) and (4) into Equation (8) and Equations (1) and (5) into Equation (9) and solving for the half-fracture length, the following expressions are obtained, respectively,

$$x_f = 22.5632\left(\frac{qB}{h(\Delta P)_{BR}}\right)^{1.3889}\sqrt{\frac{t_{BR}}{\xi\phi c_t}\left(\frac{\mu}{k}\right)^{1.778}} \quad (10)$$

$$x_f = 5.4595\left(\frac{qB}{h(t*\Delta P')_{BR}}\right)^{1.3889}\sqrt{\frac{t_{BR}}{\xi\phi c_t}\left(\frac{\mu}{k}\right)^{1.778}} \quad (11)$$

Due to noisy data, it is better to draw a straight-line going through the bilinear flow regime and read the pressure derivative value, $(t*\Delta P')_{BR1}$ at a time of 1 hr, extrapolated if necessary. Then, Equation (16) becomes;

$$x_f = 5.4595\left(\frac{qB}{h(t*\Delta P')_{BR1}}\right)^{1.3889}\sqrt{\frac{1}{\xi\phi c_t}\left(\frac{\mu}{k}\right)^{1.778}} \quad (12)$$

When bilinear flow is not observed, fracture conductivity can be found using an expression presented by Tiab (2003);

$$k_f w_f = \frac{3.31739k}{\frac{e^s}{r_w} - \frac{1.92173}{x_f}} \quad (13)$$

2.3. Other flow regime governing equations

Tiab (1993) demonstrated that the dimensionless pressure derivative during radial flow regime takes the value of 0.5, then,

$$[t_D * P_D']_r = 0.5 \quad (14)$$

From which the permeability is solved Equation 5 is replaced into Equation (14):

$$k = \frac{70.6q\mu B}{h\left(t*\Delta P'\right)_r} \quad (15)$$

Where $(t*\Delta P')_r$ is the value of the pressure derivative during radial flow regime. Tiab (1993) also found an expression for the mechanical skin factor;

$$s = 0.5\left\{\frac{\Delta P_r}{\left(t*\Delta P'\right)_r} - \ln\left(\frac{kt_r}{\phi\mu c_t r_w^2}\right) + 7.43\right\} \quad (16)$$

Being ΔP_r the pressure drop read at any arbitrary time, t_r, during radial flow.

The governing pressure derivative equation during pseudosteady-state regime is given by:

$$\left[t_{DA} * P_D'\right]_p = 2\pi(t_{DA})_p \quad (17)$$

As indicated by Tiab (1994), an equation for the determination of drainage area, *A*, is found from the intersection point of the radial flow regime governing equation, Equation (14), and the pressure derivative equation during pseudosteady-state, Equation (17), as follows:

$$A = \frac{kt_{rpi}}{301.77\phi\mu c_t} \quad (18)$$

Where *trpi* is the point of intersection between the radial flow pressure derivative and the pseudosteady-state pressure derivative (extrapolated) lines.

Tiab and Bettam (2007) presented the governing expressions for early bilinear and linear flow regimes for vertical fractures in natural- fractured systems;

$$P_D = \frac{2.45}{\sqrt{C_{fD}}}\left(\frac{t_{Dxf}}{\xi}\right)^{1/4} \quad (19)$$

$$P_D = \left(\frac{\pi t_{Dxf}}{\xi}\right)^{1/2} \quad (20)$$

The corresponding pressure derivatives of the above equations are:

$$t_D * P_D' = \frac{0.6125}{\sqrt{C_{fD}}}\left(\frac{t_{Dxf}}{\xi}\right)^{1/4} \quad (21)$$

$$t_D * P_D' = \frac{1}{2}\left(\frac{\pi t_{Dxf}}{\xi}\right)^{1/2} \quad (22)$$

2.3. Points of intersection

In the eventual case that bilinear flow occurs at early time, the intersection point formed by Equation (9) and Equation (22) allows obtaining an expression for estimating the half-fracture lengths as a function of the intersect time of bilinear and birradial flow regimes, t_{BLBRi},

$$k_f w_f = 10.5422\left(\frac{\omega\phi\mu c_t k^{3.5454} x_f^{6.5454}}{t_{BRBLi}}\right)^{0.22} \quad (23)$$

The intersect t_{LBRi} formed by the pressure derivative straight-line portions of the linear and birradial flow regimes, Equations (9) and (21) also leads to obtain an equation to find the half-fracture length.

$$x_f = \sqrt{\frac{kt_{LBRi}}{39.044\omega\phi\mu c_t}} \quad (24)$$

Another way to determine the half-fracture length results from the intersection of the birradial and radial, t_{RBRi}, straight-line portions of the pressure derivative given by Equations (14) and (9),

$$x_f = \frac{1}{4584.16}\sqrt{\frac{kt_{RBRi}}{\omega\phi\mu c_t}} \quad (25)$$

The intersection formed by the birradial flow regime and the late pseudosteady-state period, t_{BRPi}, given by Equations (14) and (28) results in;

$$x_f = 41.0554A^{1.3889}\left(\frac{\omega\phi\mu c_t}{kt_{BRPi}}\right)^{0.8889} \quad (26)$$

2.4. Conventional analysis

After replacing in Equation (8) the dimensionless quantities given by Equations (1) and (4), it yields;

$$\Delta P = 9.4286\frac{q\mu B}{kh}\left(\frac{k}{\omega\phi\mu c_t x_f^2}\right)^{0.36} t^{0.36} \quad (27)$$

Or,

$$\Delta P = m_{ell}t^{0.36} \quad (28)$$

Which implies that a Cartesian plot of ΔP vs. $t^{0.36}$ (for drawdown) or ΔP vs. $[(t_p+\Delta t)^{0.36} - \Delta t^{0.36}]$ (for buildup) provides a straight line which slope, m_{ell}, provides the half-fracture length,

$$x_f = \sqrt{9.4286\frac{q\mu B}{khm_{ell}}\left(\frac{k}{\omega\phi\mu c_t}\right)^{0.36}} \quad (29)$$

3. SYNTHETIC EXAMPLES

3.1. Example-1

Determine the half-fracture length using a simulated test was run for a heterogeneous reservoir with the information given below:

B_o = 1.25 bbl/STB	q = 350 STB/D
h = 100 ft	μ = 3 cp
r_w = 0.4 ft	c_t = 1x10^{-5} psi^{-1}
P_i = 5000 psi	ϕ = 20 %
k = 300 md	ω = 0.1
λ = 1x10^{-7}	x_f = 100 ft

Solution. The pressure and pressure derivative plot against time is given in Figure-3, from which a value of $(t^*\Delta P')_{BR1}$ of 7 psi was read. This value is used in Equation 12, so,

$$x_f = 5.4595\left(\frac{350(1.25)}{100(7)}\right)^{1.3889}\sqrt{\frac{1}{(0.1)(0.2)(1\times10^{-5})}\left(\frac{3}{300}\right)^{1.778}} = 105.96 \text{ ft}$$

3.2. Example-2

Figure-4 presents pressure and pressure derivative vs. time data for a bounded homogeneous reservoir using the information given below:

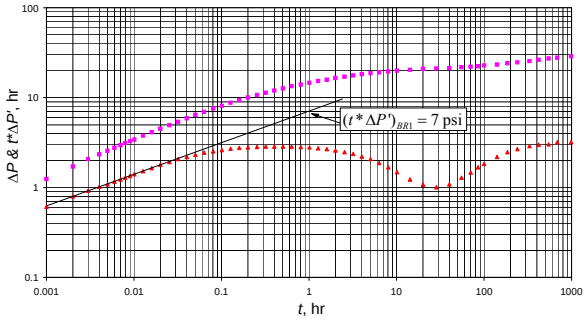

Figure-3. Pressure and pressure derivative vs. time for example-1.

B_o = 1.25 bbl/STB	q = 300 STB/D
h = 30 ft	μ = 5 cp
r_w = 0.3 ft	c_t = 3x10^{-6} psi^{-1}
P_i = 4000 psi	ϕ = 10 %
k = 33.334 md	x_f = 200 ft

It is requested for this exercise to estimate and confirm the half fracture length.

Solution. The following information was read from Figure-3,

t_{BR} = 1.01 hr $(t^*\Delta P')_{BR}$ = 64.63 t_{BRPi} = 3300 hr

Equation (12) allows estimating a half-fracture length of 199 ft and Equation (26) provides a value of 201.6 ft for the same parameter.

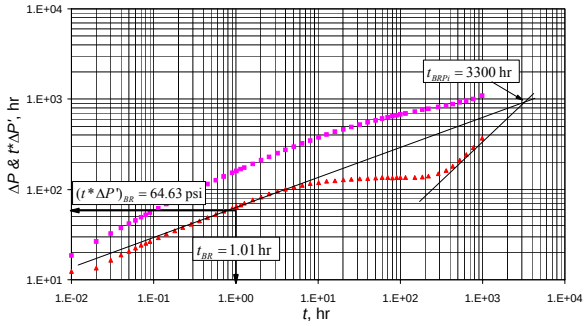

Figure-4. Pressure and pressure derivative vs. time for example-2.

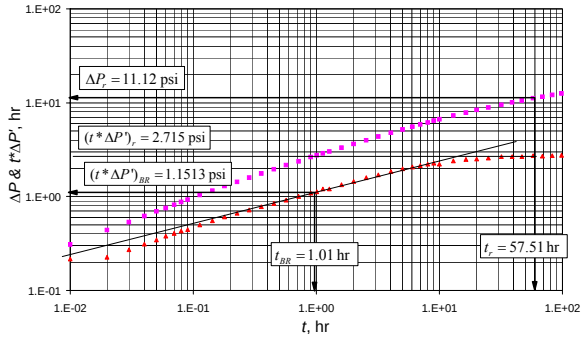

Figure-5. Pressure and pressure derivative vs. time for example-3.

3.3. Example-3

Find fracture-half length and fracture conductivity for the synthetic test which pressure and pressure derivative vs. time data is given in Figure-5. Other relevant data for this test is:

B_o = 1.1 bbl/STB q = 650 STB/D
h = 200 ft μ = 2 cp
r_w = 0.5 ft c_t = 1x10^{-5} psi^{-1}
P_i = 4000 psi ϕ = 20 %
k = 180 md x_f = 350 ft

Solution. The following information was read from Figure-3,

t_{BR} = 1.01 hr $(t^*\Delta P')_{BR}$ = 64.63 psi
t_r = 57.51 hr $(t^*\Delta P')_r$ = 2.715 psi
ΔP_r = 11.12 psi

Again, Equation (12) is used to estimate a half-fracture length of 351.1 ft. A skin factor of -5.8 is found using Equation (16). Then, Equation (13) provides a fracture conductivity value of 1'026, 606 md-ft

4. CONCLUSIONES AND RECOMMENDATIONS

A new model for the birradial/elliptical flow in fractured vertical wells is presented. The model excludes the reservoir drainage area which becomes practical in pressure tests in which the late time behavior is not observed. Both *TDS* technique and conventional analysis are used as interpretation tools. They were successfully tested with synthetic examples.

ACKNOWLEDGEMENTS

The authors thank Universidad Surcolombiana and Universidad del Atlántico for providing financial support for the complement of this study.

Nomenclature

A	Draining area, ft^2
B	Oil volume factor, rb/STB
b_x	Shortest distance from a lateral bounday to a well, ft
C_{fD}	Dimensionless fracture conductivity
c_t	Compressibility, 1/psi
h	Formation thickness, ft
k	Formation compressibility, md
$k_f w_f$	Fracture conductivity, md-ft
m	Slope
P	Pressure, psi
P_{wf}	Well-flowing pressure, psi
q	Oil flow rate, STB/D
q_g	Gas flow rate, MSCF/D
r_w	Wellbore radius, ft
Y_E	Reservoir width, ft
X_D	Dimensionless reservoir length, $2b_x/X_E$
X_E	Reservoir length, ft
x_f	Half-fracture lenght, ft
s	Skin factor
t	Test time, hr
T	Reservoir temperature, °R
$(t^*\Delta P')$	Pressure derivative, psi
$(t_D{*}P_D')$	Dimensionless pressure derivative
W_D	Dimensionless reservoir width, Y_E/r_w

Greek

Δ	Change
ϕ	Porosity, fracction
λ	Interporosity flow paramater
μ	Viscosity, cp
ξ	Variable to identify homogeneous (ξ=1) or heterogeneous (ξ=ω) reservoirs
ω	Dimensionless storativity coefficient

Suffixes

BR	Birradial
*BR*1	Birradial at 1 hr
BRBLi	Birradial-bilinear intersection
BRPi	Birradial-pseudosteady intersection
BRPBi	Birradial-parabolic intersection
BRSSi	Birradial-steady state intersection for square or circular systems
BRSS1i	Birradial-steady state intersection. Parabolic flow is seen. Far lateral boundary is at constant pressure
BRSS2i	Birradial-steady state intersection. Parabolic flow is seen. Far lateral boundary is closed
BRSS3i	Birradial-steady state intersection. Well centered in an elongated system, one lateral boundary is closed and the other one is at constant pressure
BRSS4i	Birradial-steady state intersection. Well centered in an elongated system, both lateral boundaries are at constant pressure
D	Dimensionless
DA	Dimensionless based on area
Dxf	Dimensionless based on half-fractured length
DLBRi	Dual linear-birradial intersection
ell	Elliptical
LBRi	Linear-birradial intersection
r	Radial
RBRi	Radial-birradial intersection
rpi	Intersect of radial-pseudosteady state lines
w	Well
t	Time
p	Pseudosteady-state

REFERENCES

Agarwal G. 1979. Real Gas Pseudo-time a New Function for Pressure Buildup Analysis of MHF Gas Wells. Paper SPE 8279 presented at the 54th technical conference and exhibition of the Society of Petroleum Engineers of AIME held in Las Vegas, NV, September 23-26.

Chacon A., Djebrouni A. and Tiab D. 2004. Determining the Average Reservoir Pressure from Vertical and Horizontal Well Test Analysis Using Tiab's Direct Synthesis Technique. SPE 88619, Proceedings, SPE Asia Pacific Oil and Gas Conf. and Exhibition, Perth, Australia, 18-20 October.

Cinco-Ley H., Samaniego F. and Dominguez N. 1976. Transient Pressure Behavior for a Well with a Finity-Conductivity Vertical Fracture. Paper SPE 6014 presented at the SPE-AIME 51st Annual Fall Technical Conference and Exhibition, held in New Orleans, LA, October 3-6.

Escobar F.H., Muñoz O.F. and Sepulveda J.A. 2004. Horizontal Permeability Determination from the Elliptical Flow Regime for Horizontal Wells. CT and F - Ciencia, Tecnología y Futuro. 2(5): 83-95, December.

Escobar F.H., Hernández Y.A. and Hernández C.M. 2007. Pressure Transient Analysis for Long Homogeneous Reservoirs using TDS Technique. Journal of Petroleum Science and Engineering. 58(1-2): 68-82.

Escobar F.H. and Montealegre-M M. 2008. Determination of Horizontal Permeability from the Elliptical Flow of Horizontal Wells Using Conventional Analysis. Journal of Petroleum Science and Engineering. 61: 15-20.

Escobar F.H., Hernandez Y.A. and Tiab D. 2010. Determination of reservoir drainage area for constant-pressure systems using well test data. CT and F - Ciencia, Tecnología y Futuro. 4(1): 51-72. June.

Gringarten A. C., Ramey H. J. and Raghavan R. 1974. Unsteady-State Pressure Distributions Created by a Well with a Single Infinite-Conductivity Vertical Fracture. Society of Petroleum Engineers. doi:10.2118/4051-PA. August 1.

Issaka M. B., Zaoral K., Ambastha A. K. and Mattar L. 2000. Determination of Horizontal Permeability Anisotropy from Horizontal Well Tests. This paper was prepared for presentation at the 2000 SPE Saudi Arabia Section Technical Symposium held in Dhahran, Saudi Arabia, 21-23 October.

Martinez J.A., Escobar F.H. and Bonilla L.F. 2012. Reformulation of the Elliptical Flow Governing Equation for Horizontal Wells. Journal of Engineering and Applied Sciences. 7(3): 304-313.

Tiab D. 1993. Analysis of Pressure and Pressure Derivative without Type-Curve Matching: 1- Skin and Wellbore Storage. Journal of Petroleum Science and Engineering. 12: 171-181.

Tiab D. 1994. Analysis of Pressure and Pressure Derivative without Type Curve Matching: Vertically Fractured Wells in Closed Systems. Journal of Petroleum Science and Engineering. 11: 323-333.

Tiab D. 2003. Advances in pressure transient analysis - TDS technique. Lecture Notes ManualThe University of Oklahoma, Norman, Oklahoma, USA. p. 577.

Tiab D. and Bettam Y. 2007. Practical Interpretation of Pressure Tests of Hydraulically Fractured Wells in a Naturally Fractured Reservoir. Society of Petroleum Engineers. doi:10.2118/107013-MS. January 1.

Appendix-A. Gas flow

Equations (1), (2) and (3) are applied to gas wells if the viscosity and total system compressibilities are given at initial conditions, it means $(\phi c_t)_i$. However, if those expressions are expressed using the pseudotime concept, Agarwal (1979), it yields:

$$t_{Daxf} = \frac{0.000263kt}{\phi x_f^2} t_a(P) \quad (A.1)$$

$$t_{DaA} = \frac{0.000263kt}{\phi A} t_a(P) \quad (A.2)$$

$$t_{DaL} = \frac{0.000263kt}{\phi Y_E^2} t_a(P) \quad (A.3)$$

For gas wells, Agarwal (1979) also included the pseudopressure definition,

$$m(P)_D = \frac{hk\left(m(P_i) - m(P)\right)}{1422.52 q_{sc} T} \quad (A.4)$$

which dimensionless pseudopressure derivative is given by:

$$t_D * m(P)_D{}' = \frac{hk\left(t * \Delta m(P)'\right)}{1422.52 q_{sc} T} \quad (A.5)$$

After replacing Equations (1), A.4 and A.5 into Equations (7) and (8) leads to obtain:

$$x_f = 529.16\left(\frac{q_{sc}T}{h(\Delta m(P)_{BR}}\right)^{1.3889} \sqrt{\frac{t_{BR}}{\omega\phi(\mu c_t)_i k^{1.778}}} \quad (A.6)$$

$$x_f = 138.687\left(\frac{q_{sc}T}{h(t * \Delta m(P)'_{BR}}\right)^{1.3889} \sqrt{\frac{t_{BR}}{\omega\phi(\mu c_t)_i k^{1.778}}} \quad (A.7)$$

$$x_f = 138.687\left(\frac{q_{sc}T}{h(t * \Delta m(P)'_{BR1}}\right)^{1.3889} \sqrt{\frac{1}{\omega\phi(\mu c_t)_i k^{1.778}}} \quad (A.8)$$

For the case of using the pseudotime function and replacing Equation A.1 instead of Equation 1 into Equations 7 and 8 allows obtaining:

$$x_f = 529.16\left(\frac{q_{sc}T}{h(\Delta m(P)_{BR}}\right)^{1.3889} \sqrt{\frac{t_a(P)_{BR}}{\omega\phi k^{1.778}}} \quad (A.9)$$

$$x_f = 138.687\left(\frac{q_{sc}T}{h(t * \Delta m(P)'_{BR}}\right)^{1.3889} \sqrt{\frac{t_a(P)_{BR}}{\omega\phi k^{1.778}}} \quad (A.10)$$

$$x_f = 138.687\left(\frac{q_{sc}T}{h(t * \Delta m(P)'_{BR1}}\right)^{1.3889} \sqrt{\frac{1}{\omega\phi k^{1.778}}} \quad (A.10)$$

In conventional analysis for gas flow case, Equation (7) becomes,

$$\Delta P = 94.989 \frac{q_g T}{kh}\left(\frac{k}{\omega\phi\mu c_t x_f^2}\right)^{0.36} t^{0.36} \quad (A.11)$$

Then, the slope of the Cartesian plot will give,

$$x_f = \sqrt{94.989 \frac{q_g T}{khm_{ell}}\left(\frac{k}{\omega\phi\mu c_t}\right)^{0.36}} \quad (A.12)$$

Appendix-B. Elongated systems

Escobar, Hernandez and Hernández (2007) presented the pressure solution for dual-linear, single-linear and parabolic flow regimes which take place in elongated reservoirs. Their pressure derivatives are, respectively,

$$(t_D * P_D{}')_{DL} = \sqrt{\pi t_{D_L}} \quad (B.1)$$

$$(t_D * P_D{}')_L = \pi\sqrt{t_{D_L}} \quad (B.2)$$

$$t_D * P'_D = \frac{W_D}{2} X_D^2 \left(\frac{X_E}{Y_E}\right)^2 t_D^{-0.5} \quad (B.3)$$

where the dimensionless reservoir length and width are given as follows:

$$X_D = \frac{2b_x}{X_E} \quad (B.4)$$

$$W_D = \frac{Y_E}{r_w} \quad (B.5)$$

When parabolic flow takes place and if the test is long enough state-state develops. The governing pressure derivative expressions when the far boundary is either at constant pressure or close boundary are given below:

$$t_D * P_D{}' = \left(\frac{W_D^2}{\pi^2}\right)\left(X_D^{1.5}\right)\left(\frac{X_E}{Y_E}\right)^3 (t_D^{-1}) \quad (B.6)$$

$$t_D * P_D{}' = \left(\frac{W_D^2}{\pi}\right)\left(X_D^{1,5}\right)\left(\frac{X_E}{Y_E}\right)^3 (t_D^{-1}) \quad (B.7)$$

Escobar, Hernandez and Tiab and (2010) presented the governing Equations for rectangular systems

with one or both lateral boundaries being under constant-pressure conditions. The governing equation of the negative unit slope tangential to the pressure derivative curve for a well centered inside a rectangular reservoir with one constant-pressure boundary is given here as:

$$t_D * P_D' = \frac{32 W_D^2}{19\pi}\left(\frac{X_E}{Y_E}\right)^3 t_D^{-1} \quad \text{(B.8)}$$

When both lateral boundaries are subjected to constant pressure, the governing equation of the negative unit slope tangential to the pressure derivative curve is given as:

$$t_D * P_D' = \frac{W_D^2}{5\pi}\left(\frac{X_E}{Y_E}\right)^3 t_D^{-1} \quad \text{(B.9)}$$

As far as elongated systems is concerned, the intersect point formed by Equation (9) with Equations B.1, B.2 and B.3 and B.6-B.9 provided the below expressions.

Intersect of birradial and Dual Lineal, t_{DLBRi},

$$x_f = \frac{0.7787}{\sqrt{\xi}}\left(\frac{\phi\mu c_t}{k t_{DLBRi}}\right)^{\frac{7}{36}} Y_E^{\frac{25}{18}} \quad \text{(B.10)}$$

Corte birradial y single-Lineal, t_{SLBRi},

$$x_f = \frac{Y_E^{\frac{25}{18}}}{2.8412\sqrt{\xi}}\left(\frac{\phi\mu c_t}{k t_{SLBRi}}\right)^{\frac{7}{36}} \quad \text{(B.11)}$$

Intersect of birradial and parabolic, t_{BRPBi},

$$x_f = \frac{\left(\frac{k t_{BRPBi}}{\phi\mu c_t}\right)^{\frac{43}{36}} Y_E^{\frac{25}{18}}}{141838.4826\sqrt{\xi} b_x^{25/9}} \quad \text{(B.12)}$$

Intersect of birradial and steady state, t_{BRSS1},

$$x_f = \frac{1}{2918844.802}\frac{\left(\frac{k t_{BRSS1i}}{\phi\mu c_t}\right)^{\frac{17}{9}} Y_E^{\frac{25}{18}}}{\sqrt{\xi}\left(b_x X_E\right)^{\frac{25}{12}}} \quad \text{(B.13)}$$

Intersect of birradial and steady state, t_{BRSS2},

$$x_f = \frac{1}{14311888.3}\frac{\left(\frac{k t_{BRSS2i}}{\phi\mu c_t}\right)^{\frac{17}{9}} Y_E^{\frac{25}{18}}}{\sqrt{\xi}\left(b_x X_E\right)^{\frac{25}{12}}} \quad \text{(B.14)}$$

Escobar *et al*. (2007) introduced tan approximation for the dimensionless pressure derivative of square and circular shaped systems under steady-state period,

$$t_D * P_D' \approx \frac{\pi}{84 t_{DA}} \quad \text{(B.15)}$$

Intersect of birradial, Equation (14), and steady state, Equation (52), for circular or square systems, t_{BRSSi}, leads to,

$$x_f = \frac{1}{172549.1653}\frac{\left(\frac{k t_{BRSSi}}{\phi\mu c_t}\right)^{\frac{17}{9}}}{\sqrt{\xi} A^{25/18}} \quad \text{(B.16)}$$

Intersect of birradial and steady state for a centered well in a rectangular system with a constant-pressure lateral boundary, t_{BRSS3},

$$x_f = \frac{1}{6972056.52\sqrt{\xi} X_E^{4.1667}}\left(\frac{k t_{BRSS3i}}{\phi\mu c_t}\right)^{\frac{17}{9}} \quad \text{(B.17)}$$

Intersect of birradial and steady state for a centered well in a rectangular system with both constant-pressure lateral boundaries, t_{BRSS4},

$$x_f = \frac{1}{361517.91\sqrt{\xi} X_E^{4.1667}}\left(\frac{k t_{BRSS4i}}{\phi\mu c_t}\right)^{\frac{17}{9}} \quad \text{(B.18)}$$